SAND2007-3280C

Alloy Depletion and Martensite Formation During Glass-to-Metal Joining of Austenitic Stainless Steels

D. F. Susan[1], M. J. Perricone[2], C. V. Robino[1], J. R. Michael[1], B. B. McKenzie[1], and M. Rodriguez[1]
*1. Sandia National Laboratories, Albuquerque, NM, USA
2. Formerly with Sandia, RJ Lee Group, Inc., Monroeville, PA, USA

Keywords: Joining, Oxidation, Glass, Stainless Steel, Martensite

Abstract

Pre-oxidized and glass-to-metal (GtM) sealed austenitic stainless steels were found to display a ferritic layer near the metal/oxide interface, as determined by electron backscatter diffraction (EBSD). Electron probe microanalysis (EPMA) showed that this layer was depleted in alloying elements due to the oxidation and sealing process. Characterization of the morphology suggested that it formed through the martensite transformation mechanism. Moreover, this observed layer was correlated to the composition gradient through published empirical relationships for martensite-start (M_s) temperatures. Due to Cr, Mn, and Si depletion during pre-oxidation and glass sealing, M_s temperatures near room temperature are possible in this surface region. Further support for a martensitic transformation was provided by thermochemical modeling. Possible detrimental ramifications of bulk composition, surface depletion, and phase transformations on GtM sealing are discussed.

*Sandia is a multiprogram laboratory operated by Sandia Corporation, a Lockheed Martin Company, for the United States Department of Energy's National Nuclear Security Administration under contract DE-AC04-94AL85000.

Introduction

An oxidation treatment, also called "pre-oxidation", is often performed prior to glass/metal joining to provide a transition layer -- a chromium-rich oxide in the case of stainless steel -- which bonds chemically to both the metal and the glass. In some applications, the necessary oxidation can be achieved during heating to the sealing temperature, thereby eliminating a separate pre-oxidation step. During pre-oxidation of austenitic stainless steel, thin (~1 micron) layers of oxide containing Cr, Mn, and Si are grown on the alloy surface [1,2]. The pre-oxidation treatment is performed in a low pO_2 atmosphere to avoid iron-oxide formation, which has been found to be detrimental to glass bonding. Detailed discussions of glass/metal sealing and pre-oxidation can be found elsewhere [3-6].

Depending on the duration and temperature of the pre-oxidation treatment, the surface of the alloy may become depleted in the elements that undergo an oxidation reaction. This surface chemistry change can lead to phase transformations near the alloy surface during high temperature processing or upon cooling [7-10]. The objectives of the present work were to characterize the surface depletion layer in 304L stainless steel and its effects on alloy phase transformations. In particular, the appearance of a layer with body-centered cubic (BCC) crystal structure at the stainless steel surface will be investigated. The possible martensitic origins of this

near-surface layer will be analyzed and a brief outline of the ramifications of this phase transformation on glass adhesion to 304L stainless steel will be presented.

Experimental Procedure

Several heats of 304L stainless steel were characterized after pre-oxidation at 1000, 1050, and 1095˚C for 30 to 90 minutes in a low pO_2 atmosphere. In addition, samples were also analyzed after subsequent glass sealing operations at 920-970˚C in an N_2/H_2 atmosphere, holding long enough for glass flow and seal formation. Detailed descriptions of the pre-oxidation and glass joining processes are contained elsewhere [1,2].

X-ray diffraction (XRD) experiments were performed to study oxide phase formation and alloy crystal structure before and after high temperature exposure. Sequential high temperature XRD experiments were also conducted to investigate the formation of oxide and alloy phases *in situ*. The heating rate between test temperatures was 200˚C/min in these XRD experiments. Hold time at each temperature was approximately 2 minutes for the completion of the XRD scans. The experiments were performed with the 304L samples attached to a heated XRD stage in a helium atmosphere. The oxygen partial pressure, pO_2, of the gas was sufficient to oxidize the active elements (Cr, Mn), while avoiding iron oxide formation. In this respect, although the XRD atmosphere was different than the usual pre-oxidation runs, the observed oxide phases demonstrated that sufficient similarity exists between the two oxidation conditions to draw conclusions about the usual pre-oxidation treatments based on the XRD results.

To prepare for microstructural characterization and chemical microanalysis, the 304L samples were cross-sectioned and polished using standard metallographic procedures. Electron probe microanalysis (EPMA) was performed to quantitatively characterize local alloy composition, with EPMA traces performed normal to the metal surface into the bulk alloy using 0.5 micron steps. Electron backscatter diffraction (EBSD) was used to analyze the crystal structure in the alloy near the surface after pre-oxidation and glass sealing treatments. With the combination of EPMA and EBSD identification of the BCC phase near the metal/oxide interface, the relationship between chemistry and crystal structure was established. These results were correlated to published empirical equations for martensite-start (M_S) temperatures.

Results and Discussion

Surface Alloy Depletion and Phase Transformation During GtM Seal Processing

After pre-oxidation, a layer of body-centered-cubic material (ferrite) was observed near the 304L surface, just below the oxide layers. Figure 1 shows EBSD results from a 304L sample after oxidation at 1095˚C for 90 minutes. A thin layer (~ 3 to 5 microns deep) of ferrite is shown just below the oxidized surface. Three possible mechanisms were considered for the formation of this layer: 1) diffusional transformation at high temperature due to alloy depletion of Mn (a strong γ-austenite stabilizer) caused by Mn,Cr-oxide spinel formation, 2) diffusional formation of δ-ferrite during cooling, or 3) martensitic (γ-austenite to martensite) transformation during cooling. Mechanisms 2 and 3 are also influenced by the alloy depletion layer near the surface, defined by changes in Cr, Mn, and/or Si concentration. With regard to mechanism 1, several

studies have shown diffusional formation of ferrite layers during oxidation of low Ni stainless steels, Fe-Cr-Mn-Al alloys, and other austenitic alloys [7-10]. These surface layers typically display planar interfaces parallel to the alloy surface, typical of a layer formed by long range diffusion. Ferrite formation at high temperature might also be expected in 304L since the alloy composition is close to the austenite/(ferrite + austenite) phase boundary at 1000-1100˚C [11,12]. The formation of ferrite at high temperature has been shown to influence alloy oxidation since diffusion rates of elements such as Cr and Si are higher in δ-ferrite than in γ-austenite [9,10]. Therefore, it was initially thought that the presence of a BCC layer could be an explanation for the observed differences in oxide morphology among various heats of 304L studied previously [1,2]. However, the jagged morphology of the BCC layer (Fig. 1) suggested that this layer was a product of a martensitic reaction on cooling, although this morphological evidence is far from conclusive. However, it seems unlikely that these microstructural features are diffusional Widmanstatten, as Widmanstatten plates typically form as side-branches from allotriomorphs that form along prior austenite grain boundaries, none of which was observed here (Fig. 1). As shown below, several other factors were found which ruled out high temperature diffusional transformation as the mechanism for ferrite formation during short-term pre-oxidation.

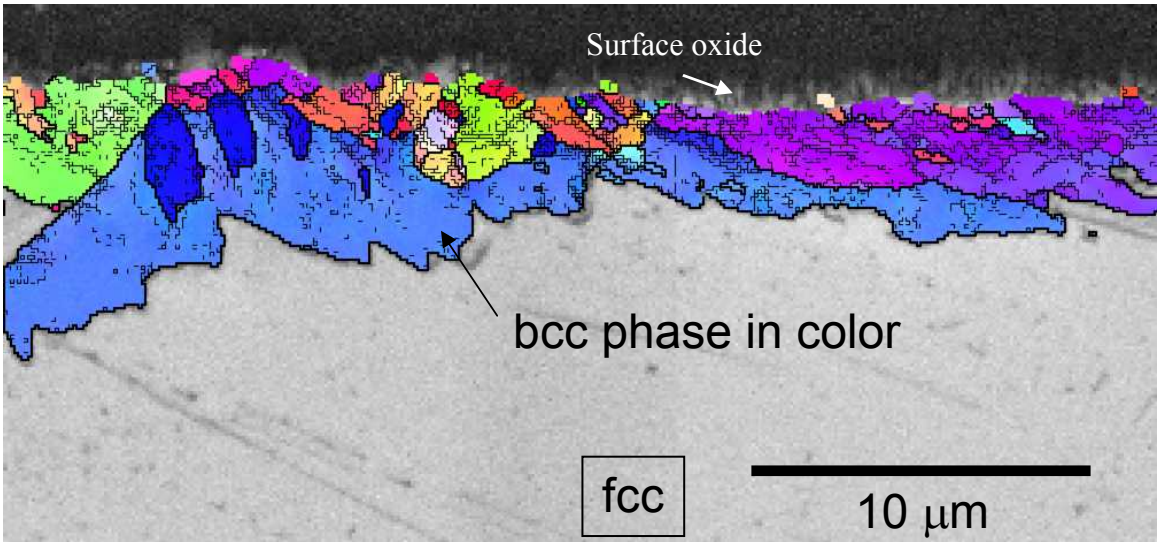

Figure 1a EBSD image of BCC phase near surface of 304L after pre-oxidation at 1095˚C, 90 min.

Figure 2a shows XRD spectra from as-received (machined from bar) 304L samples from several heats. Only γ-austenite peaks are observed, as expected. No evidence for deformation induced ε-martensite, a distinct possibility for 304L, was found in any of the as-machined samples. Figure 2b displays XRD spectra from two 304L heats after oxidation at 1000, 1050, and 1095˚C. Peaks from several oxide phases are identified including Cr_2O_3, $MnCr_2O_4$ spinel, and SiO_2 quartz. In general, the oxide phase identifications are consistent with previous results obtained by SEM, TEM, and spectrum imaging [1,2]. The relatively weak quartz peak in some spectra and its absence in other spectra suggest that SiO_2 may be present in crystalline quartz form and/or as amorphous silica. The presence of ferrite/martensite peaks in some samples after oxidation confirms the EBSD results shown above. However, the difficulty in using the XRD data in Fig. 2 to distinguish between ferrite and martensite in this alloy is that XRD cannot make that distinction due to the low amount of carbon present. However, sequential high temperature

XRD experiments were performed to determine whether the BCC phase formed at high temperature or on cooling.

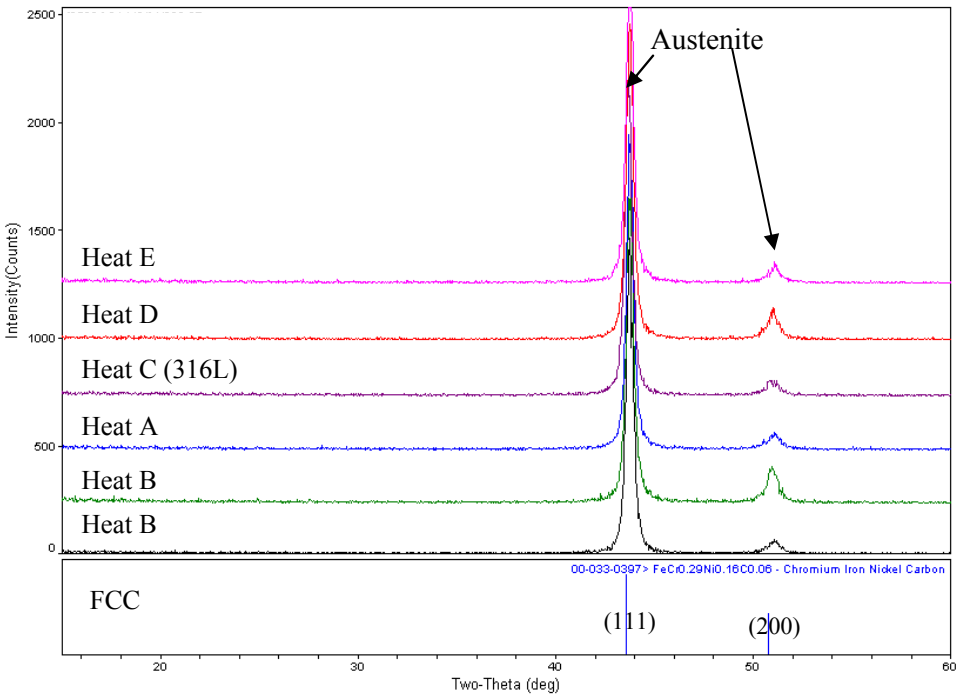

Figure 2a XRD patterns from as-machined samples prior to oxidation experiments.

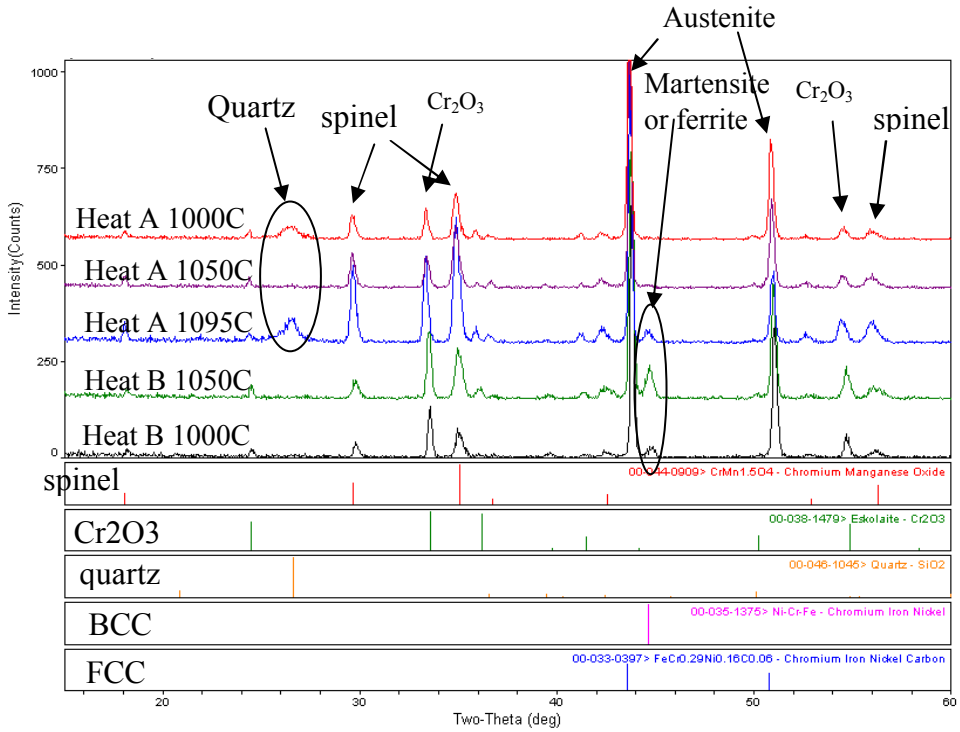

Figure 2b XRD patterns obtained after pre-oxidation at 1000, 1050, and 1095˚C for 2 heats.

Elevated temperature sequential X-ray diffraction (XRD) experiments were performed to investigate the formation of the BCC layer. The evidence from the XRD experiments shows that bcc layer formation does not occur at the pre-oxidation or sealing temperatures, but rather at some point during cooling (mechanism 2 or 3 above). Figure 3a shows in-situ XRD results on one heat of 304L for heating experiments from room temperature to 1000˚C, with a 30 min. hold at 1000˚C. Appreciable Cr_2O_3 formation (detectable as an XRD peak) begins at about 700˚C. $MnCr_2O_4$ spinel formation begins at about 900˚C. Note that the shift in the FCC peak is due to thermal expansion effects and the Pt peak is an artifact from the XRD system. No BCC peaks were found during high temperature exposure. Similar results were obtained for a 2nd heat (not shown here), with no BCC peak observed at high temperature. Another set of XRD experiments was performed with an isothermal hold for 30 minutes at 1000˚C and subsequent rapid cooling to room temperature (Fig. 3b). The XRD peaks at high temperature were similar to those shown in Fig. 3a, i.e. oxide phases and fcc-austenite. Upon cooling to room temperature, a BCC/martensite peak was detected. The XRD results in Figs. 2 and 3 clearly show that when BCC formation does occur, it does so during cooling and not at elevated temperature. However, based on the present XRD results, it is not possible to definitively determine the mechanism of BCC formation because the temperature of onset is not known.

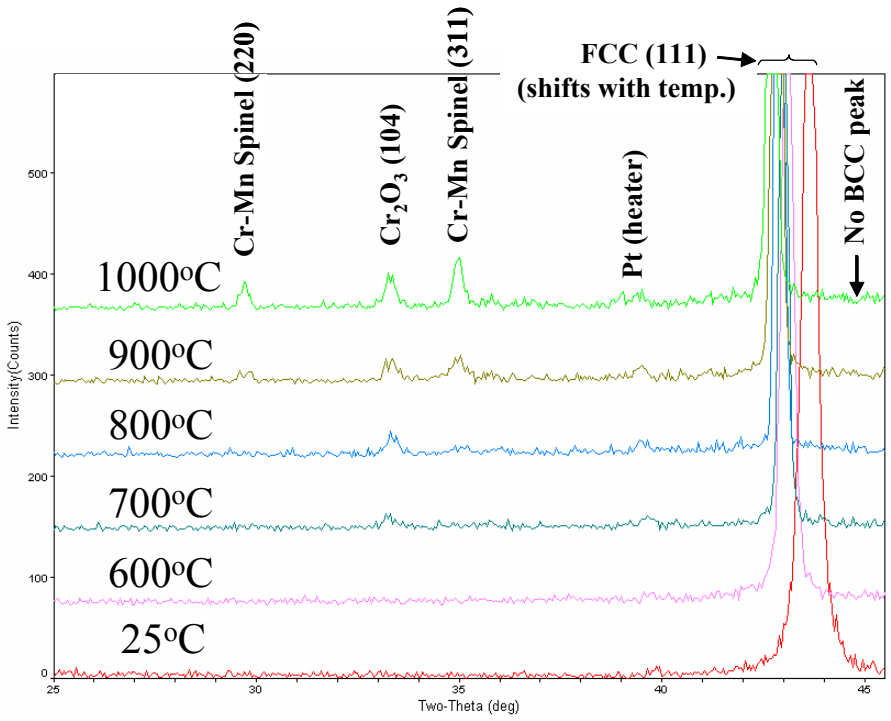

Figure 3a Sequential XRD results from heating experiment and isothermal hold at 1000˚C.

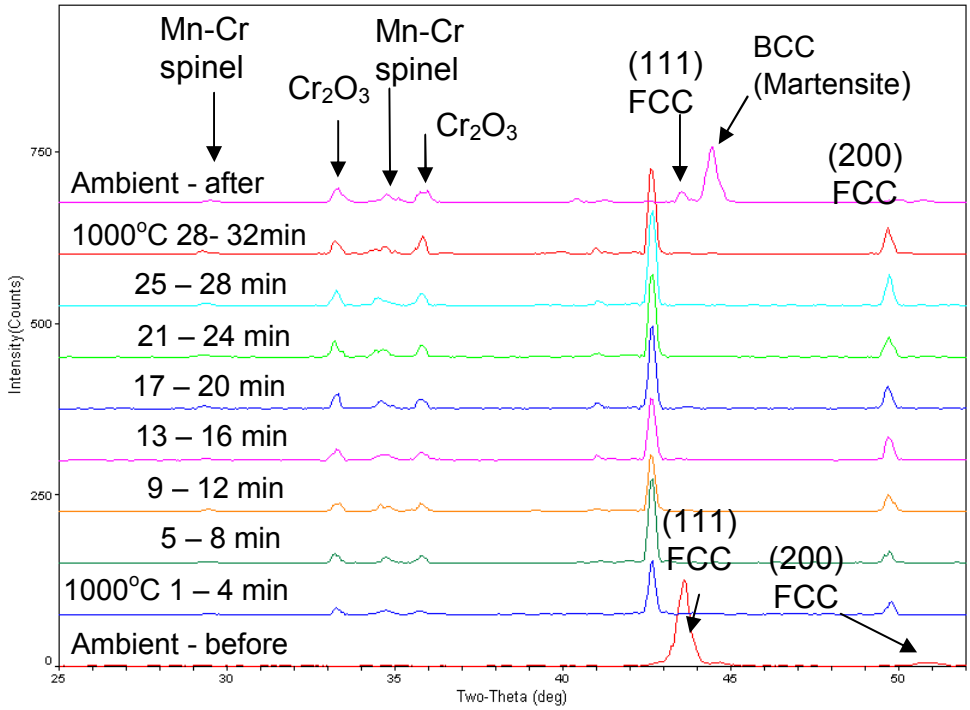

Figure 3b Sequential XRD results for 30 min at 1000˚C followed by rapid cool to room temp.

Thus, mechanisms 2 and 3 -- diffusional ferrite formation during cooling and martensitic phase transformation -- are the possible sources of the surface ferrite/martensite layer observed in oxidized samples of 304L. Future dynamic XRD experiments are planned with XRD scans performed *during cooling* to distinguish between these two possibilities. It is noteworthy that a martensitic reaction could be more detrimental to glass/metal adhesion, producing more transformation stresses than diffusional ferrite formation due to the rate of growth and low onset temperature (below the T_g of the glass). The volume expansion accompanying the FCC to BCC transformation, and the associated high stresses, were studied by Knorovsky and coworkers [13]. In addition, the formation of a surface layer of bcc material also reduces the local coefficient of thermal expansion (CTE) of the stainless steel and may decrease the magnitude of compression imparted in a "compression-type" glass-to-metal seal [13].

Thermochemical modeling with JMatPro [14] and ThermoCalc [15], to be discussed in a later publication, suggest that a martensitic transformation is possible and is a more likely scenario than diffusional ferrite formation on cooling. As shown below, correlations to empirical M_S temperature calculations indicate that martensite formation is possible at or near room temperature in the surface-depleted region.

EPMA Results and Correlations to Empirical Martensite-Start (M_S) Calculations

Figure 4 shows examples of EPMA traces perpendicular to the surface of 304L samples after pre-oxidation at 1050˚C. For ease of interpretation, only data from the elements Cr, Mn, and Si are shown in each plot, respectively. Several duplicate EPMA traces were performed on each sample to confirm the microanalysis trends. It is clear that significant depletion of these elements occurs due to diffusion and surface oxide formation. For example, the Cr concentration

drops from 18wt% in the bulk to approximately 14wt% near the surface. Slightly more severe elemental depletion was found for oxidation at 1095˚C (not shown) owing to the thicker oxide layer that forms at that temperature. The accuracy of the EPMA results is supported by comparison of the bulk concentrations in Fig. 4 with the bulk chemical analysis of this heat, found by wet chemical analysis to be 18.5wt.% Cr, 1.32wt.% Mn, and 0.53wt.% Si. These data correspond well with the EPMA measurements of the bulk material.

The alloy depletion profiles indicate that the presence of ferrite near the surface is related to the local chemistry variation in this region. It is interesting, however, that the onset of alloy depletion occurs at a depth of about 8-10 microns, but the depth of ferrite formation is only ~3-5 microns (Fig. 1). The evidence for martensite was unexpected since the usual M_S temperature for 304L stainless steel is on the order of -250˚C. The depleted alloy chemistry found at the surface in these experiments is apparently conducive to martensite formation at higher temperature (i.e. at or near ambient) upon cooling from pre-oxidation. Referring to Fig. 4, the chemistry near the surface is analogous to an alloy such as PH 13-8 Mo stainless steel (albeit with lower molybdenum content), which does exhibit M_S temperatures near room temperature.

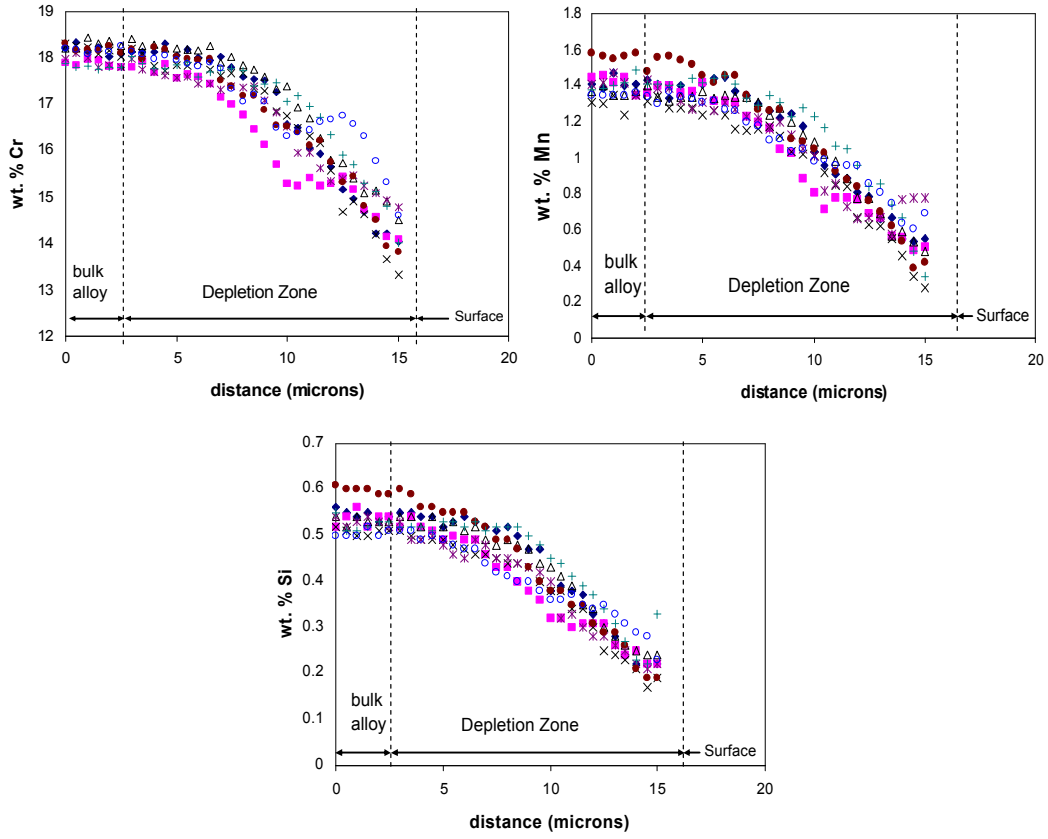

Figure 4 EPMA results from eight replicate traces showing depletion of Cr, Mn, and Si near the oxidized alloy surface of heat B after pre-oxidation at 1050˚C, 90 min.

It is also important to mention a unique aspect of this type of oxidation. Since the low pO_2 atmosphere does not allow Fe-oxide formation, no depletion of Fe occurs in the metal near the surface. The EPMA analyses confirmed that the relative Fe (as well as Ni) concentration is

locally flat or slightly increasing near the surface (not shown here). Under more common oxidation conditions, e.g. in air, Fe oxidation and surface depletion *would* occur, resulting in a different metal surface chemistry than that found in the present study. Therefore, for applications in air or other atmospheres, the surface alloy chemistry may not favor the formation of ferrite/martensite. As such, martensite formation is not usually addressed in the 304L high temperature oxidation literature.

To further support the assertion of martensite formation associated with alloy depletion, the EPMA results were used as inputs to empirical M_S temperature calculations found in the technical literature. Figure 5 shows several attempts at correlating the local composition at the surface to various M_S equations for stainless steel and low alloy steels. For the empirical formulae developed for low-alloy steels, none of the calculated M_S temperature plots gave satisfactory results. For several of the M_S equations, the bulk alloy M_S temperature was not representative of 304L. The equations of Self et al. and Payson and Savage did show reasonable M_S temperatures for bulk 304L, but the depletion layer M_S temperatures did not sensibly correlate with the observations in the present work. The wide discrepancies observed here are likely due to the alloy-specific nature of the empirical equations for M_S temperatures. Thus, each equation is only valid for a specific composition range, leading to significant variations in calculated Ms temperatures for other alloys [16]. As shown below, an equation developed by Eichelman and Hull specifically for high-Cr austenitic stainless steels correlates well to both the bulk 304L M_S temperature and the proposed martensite layer formed near ambient temperatures at the surface.

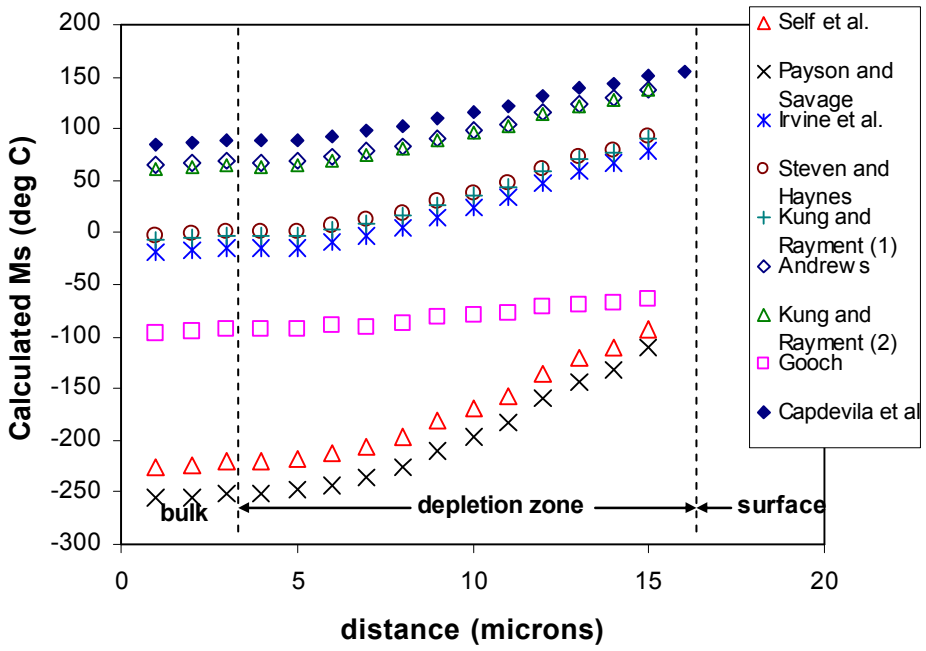

Figure 5 Calculated M_S temperatures from several empirical equations for low alloy steels. Input data are from avg EPMA trace values from heat A, 1095˚C, 90 min. (Capdevila et al. Ref. 19, other references given in Ref. 16)

In contrast to low alloy steels, fewer M_S equations are available for high-Cr austenitic stainless steels. The best approximation for M_S temperature was from the work by Eichelman and Hull [17], in which higher Cr alloys were investigated (up to ~18 wt. Cr). The Eichelman and Hull equation for M_S temperature (in ˚F) is given as follows:

$$M_S = 75(14.6 - Cr) + 110(8.9 - Ni) + 60(1.33 - Mn) + 50(0.47 - Si) + 3000(0.068 - [C + N]) \qquad \text{Eq. 1}$$

where the compositions are expressed in wt.%. The results of Eq. 1 for the depletion profile chemistries (Fig. 4) are shown in Figure 6a. The use of this equation gives reasonable values for the M_S temperature of the bulk alloy. Furthermore, the data in the depletion zone illustrate the stronger effect of chemistry variation on M_S temperature when compared to low alloy steels (Fig. 5). When Eq. 1 is used, the results indicate that the *Ms temperatures approach room temperature near the alloy surface*. A few of the M_S values calculated for the near-surface chemistries lie above room temperature while others are slightly below room temperature. Most of the M_S values near the alloy surface are within about 50˚C of room temperature, which is a compelling observation when authors have warned that the prediction differences among such empirical M_S calculations can be greater than 100˚C [16]. Consequently, the results of M_S temperature correlations show that it is possible to form martensite at the surface of 304L upon cooling after pre-oxidation under the conditions of this study.

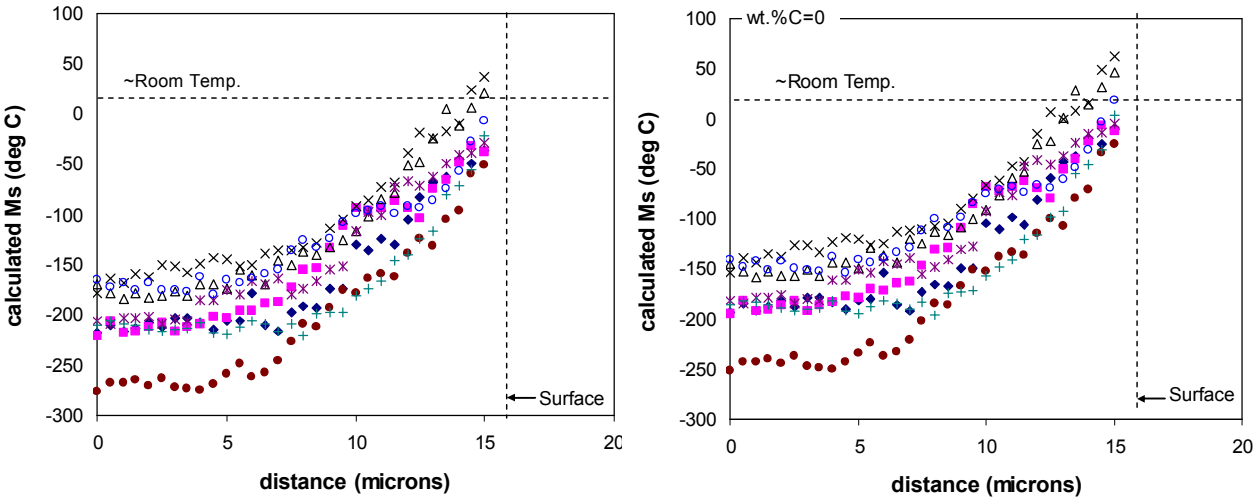

Figure 6 a) M_S temperatures calculated from several EPMA traces using Eichelman and Hull Eqn. 1 (EPMA input data from heat B, 1050˚C, 90 min (Fig. 4)), b) Calculated M_S temperatures assuming wt. % carbon = 0.

Finally, it is important to note the very strong effect of carbon (and nitrogen) on the M_S temperature in Eq. 1 as well as the other M_S equations in the literature. Even though the overall effect is minor in these alloys due to their very low carbon content, the effect of carbon was also investigated for completeness. (The bulk carbon concentration was used in Fig. 6a.) Local carbon concentration is difficult to measure with EPMA, especially in 304L in which the overall carbon content is low. However, it is likely that significant decarburization occurs during high temperature oxidation. Simple diffusion calculations suggest that carbon depletion would occur

to a depth of several hundred microns after 30 minutes at 1000-1100˚C [18]. Thus, it is likely that the carbon concentration within the alloy depletion zone (only the outer ~15 microns) essentially approaches zero. The M_S calculation in Eq. 1 was repeated assuming a carbon concentration of zero. The results (Fig. 6b) show a slight increase in the effective M_S temperatures attained near the alloy surface.

Conclusions

A layer depleted in Cr, Mn, and Si was found at the surface of 304L stainless steel after pre-oxidation and glass sealing treatments. A thin layer of bcc material was observed within this depletion layer at the alloy surface. Significant evidence was found to indicate a martensitic phase transformation on cooling was responsible for this transformed surface layer. Importantly, the EPMA data was correlated to the published M_S equation of Eichelman and Hull and M_S temperatures in the vicinity of room temperature were determined for compositions near the alloy surface. A martensitic phase transformation during cooling could have detrimental effects on glass/metal seals by producing high stresses and a change in CTE near the glass/metal interface.

Acknowledgements

The authors would like to thank P. Hlava for expert EPMA analysis, A.C. Kilgo for metallography, and C. Walker for pre-oxidation and glass sealing experiments.

References

[1] D.F. Susan, J.A. Van Den Avyle, S.L. Monroe, N.R. Sorensen, B.B. McKenzie, J.R. Michael, J.E. Christensen, and C.A. Walker, "The Effects of 304L Stainless Steel Pre-Oxidation on Bonding to Alkali Barium Silicate Glass", *Proc. 30th Int. Conf. Advanced Ceramics and Composites*, Cocoa Beach, FL, Jan. 2006.

[2] D.F. Susan, J.A. Van Den Avyle, S.L. Monroe, N.R. Sorensen, B.B. McKenzie, J.R. Michael, J.E. Christensen, and C.A. Walker, "High Temperature Oxidation of 304L Stainless Steel and its Effect on Glass-to-Metal Joining", *3rd Int. Brazing and Soldering Conference*, San Antonio, TX, ASM International, April 2006, p 104-10.

[3] I.W. Donald, "Preparation, Properties, and Chemistry of Glass- and Glass-Ceramic-to-Metal Seals and Coatings (Review)", *J. Materials Science*, **28**, 1993, p 2841-86.

[4] J.A. Pask and A.P. Tomsia, "Wetting, Surface Energies, Adhesion, and Interface Reaction Thermodynamics", in Engineered Materials Handbook, Vol. 4, Ceramics and Glasses, S.J. Schneider (Vol. Chair), R.E. Loehman (Joining Section Chair), ASM International, 1991, p 482-92.

[5] A.P. Tomsia, J.A. Pask, and R.E. Loehman, "Glass/Metal and Glass-Ceramic/Metal Seals", in Engineered Materials Handbook, Vol. 4, Ceramics and Glasses, S.J. Schneider (Vol. Chair), R.E. Loehman (Joining Section Chair), ASM International, 1991, p 493-501.

[6] C.J. Leedecke, P.C. Baird, K.D. Orphanides, "Glass-to-Metal Seals" in Electronic Materials Handbook, 1989, p 455-9.

[7] J.-G. Duh, J.W. Lee, and C.-J. Wang, "Microstructural Development in the Oxidation-Induced Phase Transformation of Fe-Al-Cr-Mn-C Alloys", *J. Mat. Sci.*, **23**, 1988, p 2649-60.

[8] J.G. Duh and J.G. Wang, "Formation and Growth Morphology of Oxidation-Induced Ferrite Layer in Fe-Mn-Al-Cr-C Alloys", *J. Mat. Sci.*, **25**, 1990, p 2063-70.

[9] F.J. Perez, M.J. Cristobal, G. Arnau, M.P. Hierro, and J.J. Saura, "High-Temperature Oxidation Studies of Low-Nickel Stainless Steel. Part I: Isothermal Oxidation", *Oxidation of Metals*, **55**, Nos.1/2, 2001, p 105-18.

[10] P. Perez, G. Garces, F.J. Perez, C. Gomez, and P. Adeva, "Influence of Chromium Additions on the Oxidation Resistance of an Austenitic Fe-30Mn-5Al Alloy", *Oxidation of Metals*, **57**, Nos. 3/4, 2002, p 339-61.

[11] J. W. Elmer, S. M. Allen, and T. W. Eagar, "Microstructural development during solidification of stainless steel alloys", *Metall. Trans. A* **20A**, 1989, p 2117-31.

[12] D. L. Olson, "Prediction of austenitic weld metal microstructure and properties", *Weld. Res. (Miami),* 1985, p 281s-295s.

[13] G.A. Knorovsky, R.K. Brow, R.D. Watkins, and R.E. Loehman, "Interfacial Debonding in Stainless Steel/Glass-Ceramic Seals", *Metal-Ceramic Joining Conference*, P. Kumar and V.A. Greenhut (Eds.), TMS, 1991, p 237-46.

[14] JMatPro, version 4.0, Sente Software Ltd., The Surrey Research Park, Guilford GU2 7YG – UK, copyright 1999-2005.

[15] Thermo-Calc Software AB, copyright Foundation of Computational Thermodynamics and Thermo-Calc Software AB, Stockholm Technology Park, SE 113-47, Stockholm, Sweden.

[16] J.C. Lippold and D.J. Kotecki, *Welding Metallurgy and Weldability of Stainless Steels*, Wiley-Interscience, 2005, p 62, 84-85.

[17] A.H. Eichelman, Jr. and F.C. Hull, "The Effect of Composition on the Temperature of Spontaneous Transformation of Austenite to Martensite in 18-8 Type Stainless Steel", *Trans. ASM*, Vol. 45, 1953, p 77-104.

[18] D.A. Porter and K.E. Easterling, *Phase Transformations in Metals and Alloys*, Chapman and Hall, 1981, p 73-75.

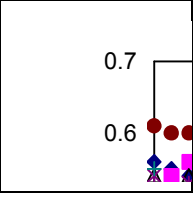

[19] C. Capdevila, F.G. Caballero, and C. Garcia de Andres, “Determination of Ms Temperatures in Steels: A Bayesian Neural network Model”, *ISIJ International*, Vol. 42, No. 8, 2002, p 894-902.